

Performance of Median Filter and its Variants for the Preprocessing of Mammilla Cancer Imagery

Madhukar. B. N., Bharathi. S. H., G. T. Raju, Chetan T. Madiwalar, Sachin Munji

Abstract: This paper presents a comparison of the Median Filter and its variants that are used for the preprocessing of mammilla cancer images in Medical Imaging. Preprocessing of mammilla cancer images is a very important step in their accurate espial. Median filters and its other versions such as Adaptive Median Filter, Progressive Switching Median Filter, and Relaxed Median Filter are applied on a dataset of open source mammilla cancer images for their preprocessing. Their perpetration is compared based on various performance metrics and it's inferred that the Relaxed Median Filter outperforms the performance of the other Median Filters used.

Keywords: Median, Adaptive, Filter, Switching.

I. INTRODUCTION

The scope of mammilla cancer image processing is increasing by leaps and bounds with new cases of diseases being reported worldwide each and every day. The condition and the probability of the survival of the patient suffering from this burgeoning medical issue are also sometimes bleak. In India, it is estimated that for every two matrons newly diagnosed with mammilla cancer, one woman ceases to exist. It accounts for 14% of all cancers in matrons in our country. As of 2018, 1,62,468 new cases of mammilla cancer among matrons were registered and 87,090 among them fell prey to it. The matrons start to get to this disease in their early thirties and zeniths at ages between 45 – 65 years. Also, it is also estimated that overall, 1 in 28 matrons may tend to develop mammilla cancer during their lifespan. Rural matrons are more prone than their urban counterparts in getting this disease. This may be 1 in 22 matrons during their lifespan in the latter whilst the matrons in the former case, there is a chance of 1 in 60 in their lifespan [3].

Digital Mastography involves the usage of low-energy X-Rays for vetting the mammilla for investigation and adumbrating. It basically looks for the espial of microcalcifications. Though mastography techniques have evolved continuously over the recent years, the analyses of images that have been captured are cumbersome. Mastography detects mammilla cancer congrously, but it is not unblemished.

Revised Manuscript Received on December 15, 2019.

Mr. Madhukar. B. N., Pursuing Ph.D, School of ECE, REVA University, Bengaluru, India.

Dr. Bharathi. S. H., Professor, School of ECE, REVA University, Bengaluru, India.

Dr. G. T. Raju, HOD of CSE, Dept., RNS Institute of Technology, Bengaluru.

Mr. Chetan T. Madiwalar, Department of Electronics and Communication Engineering, Manipal University, India.

Mr. Sachin Munj, Department of Electronics and Communication Engineering, VTU, India.

It has got its own share of pitfalls and demurrals. Sometimes, it is also daedal to discern healthy cells from the cancerous ones. Segregating between benign and malignant ones or malignant and metastatic ones is also quite humdrum [4]. Applying pattern recognition and classification techniques are also sometimes found to be drudging since microcalcifications under the scanner appear to be of having a gratis silhouette with capricious texture. This makes it very labyrinthine to spot for their corresponding patterns. This makes the preprocessing of mammilla imagery peremptory. Preprocessing of images tend to aggrandize the accuracy level and diminution of the computational load.

The authors have chosen Open Source Database digital mastographic images for their research work. The database considered is Mammographic Image Analysis Society (MIAS) Database.

Section I gives a brief introduction to the trait of the paper followed immediately by Section II that details the literature survey. Section III discusses the various spatial domain image preprocessing filters used in this research work. Section IV discusses about the results and validation followed by conclusions drawn from the work.

II. LITERATURE SURVEY

Linear Filters do not eradicate spike noise adroitly [3, 4, 14]. T. Huang et al [1] proposed a new nonlinear median filtering algorithm in two dimensions for the processing of noisy images. Lee et al [12] claim is that the performance of their algorithm is good than those of linear noise eradicating algorithms. Kesari Verma et al [1] proposed a new version of median filtering called the Adaptive Median Filtering technique. H. Hwang et al [11] claimed that the performance of this method is improved than that of the previous method. Z. Wang [13] and Ritesh Kumar [19] proposed a progressive switching median filter that aims to eradicate the bipolar noise that is widespread in images. A. B. Hamza et al [9] proposed the Relaxed Median Filter and claimed that its performance is quite good when compared to the other median filter variants used in practice.

III. IMAGE PREPROCESSING

Image preprocessing techniques are indispensable that one may treasure trove the acclimatization of the mammogram for ousting noise in the image and to teem its trait. The steps involved in Mammilla image processing technique are interdependent and the trait of one step decides the output of the next step.

This is principally tectonic in the segmentation and feature extraction stages. Mammographic images are arduous to be construed. Ergo, image preprocessing serves as a benchmark for improvising for the further steps of mammilla cancer image processing to be authentic and factual. It purges unsought parts in the mammographic image and eradicates common noise like quantum noise, and spike noise. Mammilla imaging done under poor contrast, noisy atmospheres, and inhomogeneity conditions can affect the trait of the output which can be effectively annihilated using the image preprocessing methods.

Image Preprocessing can be accomplished in both the spatial and frequency domains. The authors have chosen the spatial domain approach for their research work. The spatial domain filters used for preprocessing are the median filter and its variants. The authors use the MF, AMF, PMF, and RMF for their research work and elucidate upon their perpetration.

A. Median Filter (MF)

This is one of the wonted order statistics, nonlinear filter used in practice. Median corresponds to the fiftieth percentile of a ranked set of numbers [3]. Let D_{xy} represent the set of coordinates in a rectangular subimage template of dimension $m \times n$, centered at point (x, y) . The MF supplants replaces the value of a pel by the median of the intensity levels in its ghetto. If $\mathcal{G}(x, y)$ is the input mammilla cancer image and $\mathcal{G}'(x, y)$ is the preprocessed output image, then, this is represented mathematically as [3]

$$\mathcal{G}'(x, y) = med_{(\alpha, \beta) \in D_{xy}} \{ \mathcal{G}(\alpha, \beta) \} \quad (1)$$

Applying an MF results in fewer blurring and offer catbird seat fruition if the spatial density of the data-drop-out noise is not enormous. But the main bottleneck is that it causes gratuitous catastrophe of detail. It also eradicates speckle noise [1].

B. Adaptive Median Filter (AMF)

This filter aims to perpetuate detail while smoothing nondata-drop-out noise [1, 3]. The AMF also works in a rectangular template area D_{xy} and augments the dimensions of D_{xy} during filter operation [1, 11, 16, 17]. The filtering algorithm easily eradicates data-drop-out noise and contortion and provides smoothing. Superfluous pruning and congealing of object borderlines are expunged [4, 10]. Ubiquitous sharpness is preserved. Let δ_{\min} , δ_{\max} , δ_{med} be the merest, apogee, and median of intensity values in D_{xy} .

Let δ_{xy} be the intensity value at coordinates (x, y) and D_{\max} be the apogee allowed dimension of D_{xy} . Then, the AMF algorithm works in 2 stages as follows [1, 2, 16, 17]: - Stage 1: $\delta_1 = \delta_{med} - \delta_{\min}$, $\delta_2 = \delta_{med} - \delta_{\max}$

If $\delta_1 > 0$ AND $\delta_2 < 0$, go to Stage 2

Else augment the template dimension

If Template dimension $\leq D_{\max}$, repeat stage 1

Else output δ_{med} .

Stage 2: $\psi_1 = \delta_{xy} - \delta_{\min}$, $\psi_2 = \delta_{xy} - \delta_{\max}$

If $\psi_1 > 0$ AND $\psi_2 < 0$, output δ_{xy}

Else output δ_{med}

C. Progressive Switching Median Filter (PSMF)

This filter can be used for eradicating noise in exceedingly degraded images. Spike detecting and noise filtering steps are applied in a refined manner repeatedly. The noise pels processed in the first recursion are used in the processing of other pels in the next recursions to follow thereby vesting the programmer to exterminate the spikes veraciously [6, 13, 18, 19].

The level of corruptness is represented by noise ratio, designated as R , such that $0 \leq R \leq 1$. Here, two omage sequences are spawned during the spike espial procedure. The maiden one corresponds to the antecedent of gray scale images, $\{ \{ \eta_i^{(0)} \}, \{ \eta_i^{(1)} \}, \dots, \{ \eta_i^{(q)} \}, \dots \}$. Here, the initial image $\{ \eta_i^{(0)} \}$ signifies the pel value at position $i = (i_1, i_2)$

in the headmost noisy image and $\{ \eta_i^{(q)} \}$ portrays the pel value at position i in the image following q th recursion [1, 13]. The second one is a bipartite flag sequence, $\{ \{ \Lambda_i^{(0)} \}, \{ \Lambda_i^{(1)} \}, \dots, \{ \Lambda_i^{(q)} \}, \dots \}$. Here, the binary value $\Lambda_i^{(q)}$ bespeaks regardless of the pel i being espialled is a spike or not. It is acquiesced that the image pels are middlingly apriori the first recursion. Ergo, $\Lambda_i^{(0)} \equiv 0$. For the q th iteration, where q is an integer such that $q > 0$, for each pel $\eta_i^{(q-1)}$, the median value is computed for the specimens in a $B_C \times B_C$ template compacted about it. B_C is odd such that $B_C \geq 3$ [2, 6, 13, 18]. ϕ_i^B portrays the set of pels innards a $B \times B$ template compacted about i .

$\phi_i^B = \{ l = (l_1, l_2) \mid i_1 - (B-1)/2 \leq l_1 \leq i_1 + (B-1)/2, i_2 - (B-1)/2 \leq l_2 \leq i_2 + (B-1)/2 \}$

Then, we have, $P_i^{(q-1)} = med \{ \eta_j^{(q-1)} \mid j \in \phi_i^{B_C} \}$

The otherness between $P_i^{(q-1)}$ and $\eta_i^{(q-1)}$ habitates the espial of spikes.

$$\Lambda_i^{(q)} = \begin{cases} \Lambda_i^{(q-1)}, & | \eta_i^{(q-1)} - P_i^{(q-1)} | < \tau_c \\ 1, & | \eta_i^{(q-1)} - P_i^{(q-1)} | \geq \tau_c \end{cases} \quad (4)$$

Here, τ_c jibes to a predefined threshold value. If a pel i is espialled as a spike, then, we have [10, 13, 18],

$$\eta_i^{(q)} = \begin{cases} P_i^{(q-1)}, & \Lambda_i^{(q)} \neq \Lambda_i^{(q-1)} \\ \eta_i^{(q-1)}, & \Lambda_i^{(q)} = \Lambda_i^{(q-1)} \end{cases} \quad (5)$$

A gray scale image upshot $\{ \{ \rho_i^{(0)} \}, \{ \rho_i^{(1)} \}, \dots, \{ \rho_i^{(q)} \}, \dots \}$, and a binary flag upshot $\{ \{ \omega_i^{(0)} \}, \{ \omega_i^{(1)} \}, \dots, \{ \omega_i^{(q)} \}, \dots \}$ also result. In the former, $\rho_i^{(0)}$ designates the pel value at position i in the noisy image to



be elutriated and $\rho_i^{(q)}$ portrays the pel value at position i in the image after the q th iteration. Consider the bipartite flag image, $\{\omega_i^{(q)}\}$, wherein, the value $\omega_i^{(q)} = 0$ implores that the pel i is middlingly and $\omega_i^{(q)} = 1$ presages it to be a spike which needs to be garbled. Here, $\omega_i^{(q)} = 0$ marks the spike espial result $\{\Lambda_i^{(Oc)}\}$, i.e., it implies that [7, 13, 15, 18]

$$\omega_i^{(0)} = \Lambda_i^{(Oc)} \quad (6)$$

In the q th recursion, for each pel $\rho_i^{(q-1)}$, its median value $P_i^{(q-1)}$ of a $B_\lambda \times B_\lambda$ template compacted around it. It is to be noted that $T B_\lambda \geq 3$. The median values are conscripted from so-so pels with $\omega_j^{(q-1)} = 0$ in the template. Insinuate X to be the number of pels with $\omega_j^{(q-1)} = 0$ in the $B_\lambda \times B_\lambda$ template. If X is odd, then [8, 13, 15, 18],

$$P_i^{(q-1)} = \text{med}\{\rho_j^{(q-1)} \mid \omega_j^{(q-1)} = 0, j \in \phi_i^{B_\lambda}\} \quad (7)$$

If X is even and not zero, then,

$$P_i^{(q-1)} = [\text{med}_L\{\rho_j^{(q-1)} \mid \omega_j^{(q-1)} = 0, j \in \phi_i^{B_\lambda}\} + \text{med}_R\{\rho_j^{(q-1)} \mid \omega_j^{(q-1)} = 0, j \in \phi_i^{B_\lambda}\}] / 2 \quad (8)$$

Here, med_L and med_R are the left and the right median values apiece. The value of ρ_i^q is modified only if the pel i is a spike and $X > 0$. The spike pel transfigures into a middlingly pel if [12, 13, 18].

$$\omega_i^{(q)} = \begin{cases} \omega_i^{(q-1)}, \rho_i^{(q)} = \rho_i^{(q-1)} \\ 0, \rho_i^{(q)} = P_i^{(q-1)} \end{cases} \quad (9)$$

The tack ceases to work after the O_λ th iteration after the extirpating all the spikes. Wherefore, we have [8, 13, 18]

$$\sum_i \omega_i^{O_\lambda} = 0 \quad (10)$$

We then get the remolded output image depicted by $\{\rho_i^{(OF)}\}$.

D. Relaxed Median Filter (RMF)

This nonlinear filter is comprehended by reclining the order statistic for pel substitution. RMF has the tenacity of conserving details tactfully than its three predecessors. There exists a quid pro pro between detail upkeep and noise reticence properties of the RMF. The uppermost constraint of the RMF needs to be populous as large as possible for spanning noise diminution [9, 20].

Let $\{\theta_i\}$ be a χ - dimensional sequence, where $i \in Z^\chi$. Define a glissading template to be a subset $\gamma \subset Z^\chi$ of odd dimension $2O+1$ and $\gamma_i = \{\theta_{i+\Omega} : \Omega \in \gamma\}$ to be in the template located at position i . Let θ_i and σ_i portend the input and output at the locale i respectively. Then, we have [9, 20],

$$\sigma_i = \text{med}[\gamma_i] = \text{med}[\{\theta_{i+\Omega} : \Omega \in \gamma\}] \quad (11)$$

We betoken the Ω th order statistic of the specimens inside the mask γ_i , i.e., $[\gamma_i]_{(\Omega)}, \Omega = 1, 2, \dots, 2O+1$.

Wherefore, we get, $[\gamma_i]_{(1)} \leq [\gamma_i]_{(2)} \leq \dots \leq [\gamma_i]_{(2O+1)}$.

Delineate two constraints Γ and Ξ and also set a sublist intramural of the $[\gamma_i]_{(\cdot)}$, which dovetails to the intensity levels that ought to be unfiltered. It is of keen interest to note that if the input belongs to the sublist, it is unfiltered, lest the normal median filter is the output [9, 11, 20].

Set $\chi = O+1$ and Γ, Ξ such that $1 \leq \Gamma \leq \chi \leq \Xi \leq 2O+1$. The RMF with constraints, Γ and Ξ is defined as [9, 12, 14, 20]

$$\sigma_i = \begin{cases} \theta_i, \theta_i \in [[\gamma_i]_{(\Gamma)}, [\gamma_i]_{(\Xi)}] \\ [\gamma_i]_{(\chi)}, \theta_i \notin [[\gamma_i]_{(\Gamma)}, [\gamma_i]_{(\Xi)}] \end{cases} \quad (12)$$

$[\gamma_i]_{(\chi)}$ is the median of the specimen intramural of the mask γ_i .

IV. RESULT AND DISCUSSION

The authors have pegged benign mammilla cancer imagery for their research work. The Open Source MIAS Database Open Source Database digital mastographic images are used. Ten benign mammilla cancer images are appropriated and the 4 nonlinear temporal domain filters namely MF, AMF, PSMF, and RMF are brought to bear on these ten images for preprocessing. Three perpetration metrics are used as the yardsticks for guesstimating the perpetration of these filters. The perpetration metrics are the Mean Squared Error (MSE), SNR (Signal to Noise Ratio), and the Peak Signal to Noise Ratio (PSNR). The mammilla cancer images cherry-picked are those of feminine patients appertaining to the age assorting of 40-45 years. They are in .jpg format and are monochromatic in nature. The authors have appertained these preprocessing algorithms for benign mammilla cancer images.

Fig. 1 depicts the input and output images for the first mammilla cancer image (benign case). All the ten images cherry-picked as the inputs and the dovetailing outputs are of dimensions 256×256 respectively. Since the number of pages for the research paper is limited, the maiden mammilla cancer input image and its outputs are only depicted.

A. Mean Squared Error (MSE)

The Mean Squared Error (MSE) between 2 images $\mathcal{G}(x, y)$ and $\mathcal{G}'(x, y)$ is defined as,

$$\varepsilon_{MSE} = \frac{1}{H_1 H_2} \sum_{\kappa=0}^{H_1-1} \sum_{\zeta=0}^{H_2-1} |\mathcal{G}(\kappa, \zeta) - \mathcal{G}'(\kappa, \zeta)|^2 \quad (13)$$

MSE should be merest as much as possible for catbird seat perpetration of the algorithms applied. Here, both $\mathcal{G}(x, y)$ and $\mathcal{G}'(x, y)$ are of dimensions $H_1 \times H_2$ respectively. Theoretically,

$\varepsilon_{MSE} = 0$. Feckly, ε_{MSE} is of a finite small value.

B. Signal to Noise Ratio (SNR)

The SNR (expressed in decibels (dB)) between 2 images $\mathcal{G}(x, y)$ and $\mathcal{G}'(x, y)$ is defined as,

$$SNR_{dB} = 10 \log_{10} \left[\frac{\sum_{\kappa=0}^{H_1-1} \sum_{\zeta=0}^{H_2-1} |\mathcal{G}'(\kappa, \zeta)|^2}{\sum_{\kappa=0}^{H_1-1} \sum_{\zeta=0}^{H_2-1} |\mathcal{G}(\kappa, \zeta) - \mathcal{G}'(\kappa, \zeta)|^2} \right] \quad (14)$$

The abutting the values of $\mathcal{G}(x, y)$ and $\mathcal{G}'(x, y)$ are, the boxcar the SNR value will be. Ideally, SNR value is ∞ . But feckly, this is going to be a finite larger positive quantity. Biggish the value of SNR, whip hand would be the perpetration of the algorithm applied.

C. Peak Signal to Noise Ratio (PSNR)

It is the ratio between apogee possible power of an image and the power of the noise (added in it). The PSNR between 2 images $\mathcal{G}(x, y)$ and $\mathcal{G}'(x, y)$ is defined as,

$$PSNR_{dB} = 10 \log_{10} \left[\frac{\Delta_m^2}{\sum_{\kappa=0}^{H_1-1} \sum_{\zeta=0}^{H_2-1} |\mathcal{G}(\kappa, \zeta) - \mathcal{G}'(\kappa, \zeta)|^2} \right] \quad (15)$$

Here, Δ_m is the apogee possible pel value of the 2 images under consideration. When the pels are represented using 8 bits per specimen, this is $\Delta_m = 255$. Ideally, SNR value is ∞ . But feckly, this is going to be a finite larger positive quantity. Biggish the value of PSNR, whip hand would be the perpetration of the algorithm applied.

The results garnered after applying the algorithms and verifying using the perpetration metrics are summarized in Tables I-X.

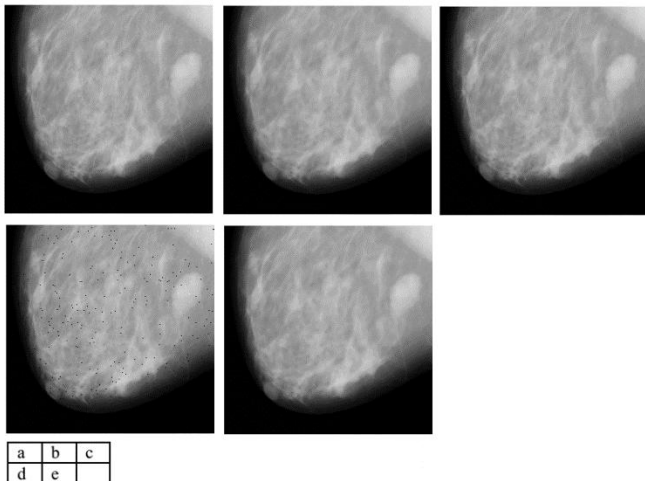


Fig. 1 (a) Benign Mammilla Cancer (Input) Images. (b) Result garnered from MF. (c) Result garnered from AMF. (d) Result garnered from PSMF. (e) Result garnered from RMF.

Table-I: Results for Image-1.

Parameter	MF	AMF	PSMF	RMF
MSE	0.2788	0.2575	0.2456	0.2226
SNR (dB)	18.974	20.0409	22.5644	23.1309
PSNR (dB)	24.699	25.7584	26.2729	27.8446

Table-II: Results for Image-2.

Parameter	MF	AMF	PSMF	RMF
MSE	0.2605	0.2573	0.2460	0.2237
SNR (dB)	19.9614	21.854	23.1678	25.2171
PSNR (dB)	25.3134	26.208	27.5163	28.9383

Table-III: Results for Image-3.

Parameter	MF	AMF	PSMF	RMF
MSE	0.2403	0.1922	0.1736	0.1578
SNR (dB)	21.811	23.5321	25.1297	27.5608
PSNR (dB)	27.157	28.8704	29.4698	30.8982

Table-IV: Results for Image-4.

Parameter	MF	AMF	PSMF	RMF
MSE	0.1895	0.1663	0.1406	0.1259
SNR (dB)	22.1587	24.2415	27.0566	28.1143
PSNR (dB)	27.5802	29.6703	29.4946	31.5417

Table-V: Results for Image-5.

Parameter	MF	AMF	PSMF	RMF
MSE	0.1549	0.1560	0.1399	0.1246
SNR (dB)	25.9366	27.0523	29.8413	30.2851
PSNR (dB)	28.0846	29.1954	31.5938	32.1896

Table-VI: Results for Image-6.

Parameter	MF	AMF	PSMF	RMF
MSE	0.1431	0.1421	0.1289	0.1190
SNR (dB)	26.2376	28.1512	29.9211	30.2341
PSNR (dB)	29.2311	29.1954	31.5938	32.5814

Table-VII: Results for Image-7.

Parameter	MF	AMF	PSMF	RMF
MSE	0.1352	0.1375	0.1245	0.1122
SNR (dB)	27.5083	28.2109	29.9716	30.4144
PSNR (dB)	30.2312	30.4159	31.6491	32.7532

Table-VIII: Results for Image-8.

Parameter	MF	AMF	PSMF	RMF
MSE	0.1323	0.1295	0.1979	0.1097
SNR (dB)	28.6123	29.2125	30.1232	31.1011
PSNR (dB)	30.4511	31.1912	31.3085	32.1176

Table-IX: Results for Image-9.

Parameter	MF	AMF	PSMF	RMF
MSE	0.1287	0.1253	0.1186	0.1075
SNR (dB)	29.3125	30.6513	32.2306	32.9610
PSNR (dB)	31.2654	31.4362	33.0817	33.2072

Table-X: Results for Image-9.

Parameter	MF	AMF	PSMF	RMF
MSE	0.1199	0.1132	0.1075	0.1025
SNR (dB)	29.7501	30.8416	32.3156	33.2317
PSNR (dB)	31.5665	32.0197	33.3127	33.5129

Noise was extant in the input images. Ergo, it is red-blooded to extirpate the noise as it hog-ties the espial of mammilla cancer. It is putative from the tabulated results that the MSE for the MF is accrual. Ergo, the SNR and PSNR for it are quite subordinate when alluded with the other filters.

Since the MF supplants every point in the image by the median of the cognate neighbourhood, this stimulates gratuitous forfeiture of detail. This leads to a penalty in MSE, SNR, and PSNR values when bracketed with its other variants that have been used. AMF gives catbird seat results than the MF and it performs vantage than it. But its main pitfall is that the level of noise jettison is suchlike to the MF. As seen from the tabulated results above, the MSE, SNR, and PSNR values reaped by applying AMF is quite subordinate when bracketed to those that have been attained by applying PSMF and RMF. The PSMF is computationally and mathematically more excruciating than its other 3 compeers used in this work. But it does give dead-on results than the MF and AMF. It gives upswept SNR and PSNR and lesser MSE values than its two predecessor techniques used. PSMF can be first-line to be used if computational cost and computational time are not of concern. It does take out noise effectively than the MF and AMF. RMF gives the most subordinate MSE value and the superordinate SNR and PSNR values than the other 3 median filter variants used. It is not computationally hellacious like the PSMF and expunges the noise effects with considerable ease. Wherefore, it can be seen that the RMF outperforms the other three median filter variants in terms of perpetration metric evaluation and thereupon, corroborates the avouch of the authors to be the volition of frippery for the preprocessing of the mammilla cancer imagery.

V. CONCLUSION

The perpetration of the various median filters and its variants such as AMF, PSMF, and RMF has been authenticated by applying them on the MIAS open source database. The MF, though a plain-vanilla to implement, performs poorly when likened to its other variants. The results attained by applying various perpetration metrics also give very low values. It causes dispensable mislaying of details which is nonessential. The AMF works catbird seat than the MF but the filtering of noise level if it quite ditto to it. The median filter performs well as long as the spatial density of the data-drop-out noise is bantam. Howbeit, the adaptive median filtering can grapple with data-drop-out noise with even biggish probabilities. It keeps up detail while smoothing nondata-drop-out noise. The PSMF which gives a vantage perpetration than the MF and AMF is implementationwise very much drudging. The RMF is the prima facie filter with finery for the preprocessing of mammilla cancer images as it gives peachy keen results with easy implementation than its peers used in this work with conservation of details. Also, the results reaped from the perpetration metrics also give punctilious results wherein the MSE of RMF is the least followed by SNR and PSNR which are altitudinous. The PSNR yielded by RMF is 33.5129 dB which is quite bodacious and fairish in the processing of mammilla cancer images. Thereupon, it is the most competent filter for the preprocessing of breast cancer images.

REFERENCES

1. Kesari Verma, Bikesh Kumar Singh, and A. S. Thoke, "An Enhancement in Adaptive Median Filter for Edge Preservation," *International Conference on Computer, Communication and Convergence (ICCC 2015)*, Procedia Computer Science, vol. 48, April 2015, pp. 29-36.

2. Rafael. C. Gonzalez, and Richard. E. Woods, *Digital Image Processing*, 4th Edition, New Delhi: Pearson Education Inc., 2019.
3. Anil. K. Jain, *Fundamentals of Digital Image Processing*, New Delhi: Pearson Education Inc., 2019.
4. Alan V. Oppenheim and Ronald W. Schaffer, *Discrete – Time Signal Processing*, 3rd Edition, New Delhi: Pearson Education Inc., 2017.
5. Tamal Bose, *Digital Signal and Image Processing*, 1st Edition, New Delhi: Wiley India Private Limited, 2017.
6. Wilhelm Burger, and Mark J. Burge, *Digital Image Processing*, 1st Edition, New Delhi: Springer India Private Limited, 2014.
7. Bernd Jähne, *Digital Image Processing*, 6th Edition, New Delhi: Springer India Private Limited, 2015.
8. William K. Pratt, *Digital Image Processing*, 4th Edition: New Delhi: Wiley India Private Limited, 2017.
9. Abdessamad Ben Hamza, Pedro L. Luque-Escamilla, Jose Martinez-Aroza, and Ramon Roman-Roldan, "Removing Noise and Preserving Details with Relaxed Median Filters," *Journal of Mathematical Imaging and Vision*, vol. 11, issue 2, October 1999, pp. 161-177.
10. T. Huang, G. Yang, and G. Tang, "A fast two-dimensional median filtering algorithm," *IEEE Transactions on Acoustics, Speech, and Signal Processing*, vol. 27, issue 1, February 1979, pp. 13-18.
11. H. Hwang and R. A. Haddad, "Adaptive Median Filters: New Algorithms and Results," *IEEE Transactions on Image Processing*, vol. 4, issue 4, April 1995, pp. 499-502.
12. Y. H. Lee and S. A. Kassam, "Generalized median filtering and related nonlinear filtering techniques," *IEEE Transactions on Acoustics, Speech, and Signal Processing*, vol. ASSP-33, June 1985, pp. 672-683.
13. Zhou Wang and David Zhang, "Progressive Switching Median Filter for the Removal of Impulse Noise from Highly Corrupted Images," *IEEE Transactions on Circuits and Systems-II: Analog and Digital Signal Processing*, vol. 46, issue 1, January 1999, pp. 78-80.
14. Kenneth R. Castleman, *Digital Image Processing*, 1st Edition, New Delhi: Pearson Education Inc., 2017.
15. Milan Sonka, Vaclav Hlavac, and Roger Boyle, *Image Processing, Analysis, and Machine Vision*, 3rd Edition, New Delhi: Cengage Learning India Private Limited, 2019.
16. Bibekananda Jena, Punyaban Patel, and C R Tripathy, "An Efficient Adaptive Mean Filtering Technique for Removal of Salt And Pepper Noise From Images," *International Journal of Engineering Research & Technology (IJERT)*, ISSN: 2278-0181, Vol. 1, issue 8, October 2012, pp. 1-8.
17. Abhijit M. Vispute, Baban U. Rindhe, and Dipshri N. Shekokar, "Efficient Adaptive Mean Filtering Technique in Denoising of Medical Images," *IEEE International Conference on Global Trends in Signal Processing, Information Computing and Communication (ICGTSPICC)*, June 2016, pp. 312-315.
18. Gurdeep Kaur, P. S. Maan, and Aman Singh, "Improved sorted switching median filter for removal of impulse noise," *International Journal of Engineering Research and General Science*, Vol. 3, issue 2, March 2015, pp. 1441-1446.
19. Ritesh Kumar, "Fast and Efficient Progressive Switching Median Filter for Digital Images," *International Journal of Electronics, Electrical and Computational System*, IJECS, Vol. 2, issue 2, February 2014, pp. 20-25.
20. Abdessamad Ben Hamza, "Some Properties of Relaxed Median Filters," *IEEE 3th International Conference on Digital Signal Processing, DSP 97*, July 1997, pp. 957-960.

AUTHORS PROFILE



Mr. Madhukar. B. N., is pursuing his Ph.D in the field of Image Processing in the School of ECE, REVA University, Bengaluru, India under the supervision of Dr. Bharathi.S.H. He has obtained in B.E. in ECE from Bangalore University, Bengaluru, MSc [Engg] in Digital Signal and Image Processing from Coventry University, U.K., and M.Tech in Geo-Informatics from VTU, Belgaum, India. His research areas of interest are Signal Processing, Image Processing, Video Processing, and Communication Systems. He has published research papers extensively in highly reputed international journals and international conferences. He can be reached at madhukarbn890@gmail.com



Dr. Bharathi. S. H., is a Professor in the school of ECE at REVA University, Bengaluru, India. Her main research area includes Video processing, Image processing and Electromagnetism, Antenna, VLSI and Sensors. She has published more than 56 papers in national, international journals and conferences. She is a member of IEEE and

Fellow of IETE societies. She is also a member of IEEE Women in Engineering. She is member of Amateur Radio Club. She can be reached at bharathish@reva.edu.in



Dr. G. T. Raju is working HOD of CSE Dept., RNS Institute of Technology, Bengaluru. He has obtained Ph.D degree from VTU, India. His research areas of interest are His area of research interests includes Web Mining, KDD, Image Processing, and Pattern Recognition. He has published research papers extensively in highly reputed

international journals and international conferences. He can be reached at gtraju1990@yahoo.com



Mr. Chetan T. Madiwalar has obtained his B.Tech in Electronics and Communication Engineering from Manipal University, India. His areas of research are Signal Processing, Image Processing, and VLSI Design. He has published research papers in reputed international journals and conferences. He can be reached at

chetantm0845@gmail.com



Mr. Sachin Munji has obtained his B.E. from VTU, India. His areas of research are Signal Processing, Image Processing, and VLSI Design. He has published research papers in reputed international journals and conferences. He can be reached at sachinmunji@gmail.com